

# Improvement Optical and Electrical Characteristics of Thin Film Solar Cells Using Nanotechnology Techniques

Ahmed Thabet, Safaa Abdelhady, A.A. Ebnalwaled, and A. A. Ibrahim

**Abstract**—This work presents a theoretical study for the distribution of nanocomposite structure of plasmonic thin-film solar cells through the absorber layers. It can be reduced the material consumption and the cost of solar cell. Adding nanometallic fillers in the absorber layer has been improved optical, electrical characteristics and efficiency of traditional thin film solar cells (ITO /CdS/PbS/Al and SnO<sub>2</sub>/CdS/CdTe/Cu) models that using sub micro absorber layer. Also, this paper explains analysis of J-V, P-V and external quantum efficiency characteristics for nanocomposites thin film solar cell performance. Also, this paper presents the effect of increasing the concentration of nanofillers on the absorption, energy band gap and electron-hole generation rate of absorber layers and the effect of volume fraction on the energy conversion efficiency, fill factor, space charge region of the nanocomposites solar cells.

**Keywords**—Thin film, nanoparticles, nanocomposites, energy conversion, optical, plasmonic, solar cells

## I. INTRODUCTION

MAGNETIC composites challenge materials like soft magnetic ferrites and electrical steels in applications with Harnessing the sun's energy to produce electricity has proven to be one of the most promising solutions to the world's energy crisis. However, the device to convert sunlight to electricity, a solar cell, must be reliable and cost effective in order to compete with conventional sources. Several solar technologies including wafer, thin film and organic, have been researched to achieve reliability, cost-effectiveness and high efficiency with huge success for instance, crystalline Silicon has been very successful from laboratory to commercial integration, and makes up to 90% of the global PV market. Cost effectiveness can be seen in the use of less material as well as increasing energy conversion efficiency.

While wafer technology is capable of meeting the high efficiency goal, thin film can satisfy minimum material usage as well. Both goals need to be met simultaneously to enable the production of electricity at a low cost and allow high market penetration of solar electricity. Thin film solar cells are favorable because of their minimum material usage and rising efficiencies. A-Si, CdTe and CIGS are the three most widely commercialized thin film solar cells [1].

The present work was supported by Nanotechnology Research Center at Aswan University that is established by aiding the Science and Technology Development Fund (STDF), Egypt, Grant No: Project ID 505, 2009-2011.

First Author is with college of engineering in Qassim University, KSA and so, Faculty of Energy Engineering in Aswan University, Egypt (e-mail: athm@aswu.edu.eg).

CdTe solar cell usually has an absorber layer thickness of 5–10  $\mu\text{m}$  [2]. On the other side, The efficiency of CdS/CdTe thin film solar cell was about 13.4%, 7.9% and 4.7% at absorber layer thicknesses 3.5 $\mu\text{m}$ , 1 $\mu\text{m}$  and 0.5 $\mu\text{m}$  [2,3].

The efficiency of CdS/PbS thin film solar cell was about 2.16% at thickness 0.5  $\mu\text{m}$  of the absorber layer and increased up to 4.13% with further increase in the thickness up to 2 $\mu\text{m}$ . Also, The open circuit voltage, maximum current density, maximum voltage, output power density and efficiency of CdS/PbS solar cell increased with increasing the absorber layer thickness [4]. Thinning the CdTe, PbS thickness down to 1 $\mu\text{m}$  more even to sub-micrometer can, in principle, significantly reduce the material consumption and, therefore, lower the solar cell production cost and time. The reduction in the efficiencies of the previous models due to the reduction of absorber layers thickness are associated with a number of problems [3,4]. The shunting path can be more easily created in the much smaller-grain-sized 0.5  $\mu\text{m}$ -thick CdTe cell than that in the 2  $\mu\text{m}$ -thick. In case of thickness of the absorber layer is reduced, the carriers will be generated closer to the back contact and have a higher probability of back contact recombination.

The increase in recombination is closed to the interface, whenever, thin absorber layers has been occurred and have attributed to enhance the tunneling recombination. Also, the open circuit voltage decreases with decreasing the absorber layer thickness due to the large leakage current and the carrier recombination loss near to the back contact. The space-charge region reached to the CdTe back contact for 0.5 $\mu\text{m}$ -thick absorber layer in CdTe solar cell. The optical and recombination losses reached about 82% and 67% at PbS absorber layer thicknesses 0.5 $\mu\text{m}$  and 2 $\mu\text{m}$ , respectively [3,4].

A key topic in thin-film solar cell research is centered on efforts to further reduce their absorber layer thicknesses to save material and processing time and cost, as well as to benefit from higher cell voltages. Closely related to this is the development of efficient light management concepts to guarantee high absorption of the incoming light in the thin absorber layer [5,6].

The aim of this paper is enhancing efficiency and optical characteristics of absorber layers of traditional (SnO<sub>2</sub>/CdS/CdTe/Cu), (ITO/CdS/PbS/Al) thin film solar cells models by using new nanocomposites semiconductor materials. Also, improving the performance of traditional models by using

Second and Fourth Authors are with Aswan Faculty of Engineering, Aswan University, Egypt (e-mail: engsafaa33@gmail.com, draaibrahim\_eg@yahoo.com).

Third Author is with Electronics & Nano Devices lab South Valley university, Qena, Egypt (e-mail: kh\_ebnalwaled@yahoo.com).

nanoparticles technique to the absorber layer for increasing the absorption and energy band gap of the absorber layer, decreasing the reverse saturation current due to the recombination, decreasing the space-charge region, increasing electron–hole generation rate in absorber layer and increasing the energy conversion efficiency, output power density and external quantum efficiency of previous models [3,4]. Finally, it has been studied the effect of variant volume fraction of nanometallic particles on the efficiency performance of nanocomposites models.

## II. THEORETICAL AND SIMULATION MODELS

The advantage of metallic nanoparticles is their resonant nature that makes them an opportune option for solar cell applications. By tuning the plasmon resonance frequencies of the nanoparticles (that is dependent on their material, size, or distribution), one can modify spectral profiles of the absorbed power of semiconductor layer [7]. This model uses various metallic nanoparticle for improving the optical properties of the absorber layer material of thin film solar cells which result improving in the performance of thin film solar cells.

The effective dielectric constant  $\epsilon_{efi}$  of a nanocomposite absorber material (CdTe in CdS/CdTe thin film solar cell or CdS/PbS thin film solar cell) using individual nanoparticle with spherical metal inclusions can be calculated using the Maxwell-Garnet theory approximates the dielectric function of a nanocomposite with spherical metal inclusions by the equation [8,9].

$$\epsilon_{efi} = \epsilon_b \frac{(\epsilon_{mi} + 2\epsilon_b) + 2F(\epsilon_{mi} - \epsilon_b)}{(\epsilon_{mi} + 2\epsilon_b) - F(\epsilon_{mi} - \epsilon_b)} \quad (1)$$

Where,  $F$  is volume fraction.  $\epsilon_b$  is dielectric constant of the semiconductor layer material which can be describe using the Drude model as shown [10-15]

$$\epsilon_b = \epsilon_{b\infty} \left( 1 - \frac{\omega_b^2}{\omega^2 + i\omega(\gamma_{mb})} \right) \quad (2)$$

And so  $\omega$  is angular frequency of light,  $\omega_b$  is the plasma angular frequency of semiconductor layer material

$\gamma_{mb}$  is the damping frequency of semiconductor absorber layer material evaluated by the following equation

$\epsilon_{b\infty}$  is the infinity dielectric constant of semiconductor layer materials that can be determined as shown

$$\epsilon_{b\infty} = \epsilon_o \left( 1 + \frac{\omega_b^2}{(E_g)^2} \right) \quad (3)$$

Where,  $\epsilon_o$  is the permittivity of free space. Using Varshni relation temperature dependence of the bandgap in semiconductors which using in absorber or window layer can be described as [16,17]

$$E_g = E_g(0) - \frac{\alpha T^2}{\beta} \quad (4)$$

Where

$E_g(0)$  is energy band gap of semiconductor material at zero temperature

$\alpha, \beta$  are constants

$\epsilon_{mi}$  is dielectric constant of the metallic inclusion which can be describe using the Drude model as shown [18-20]

$$\epsilon_{mi} = \epsilon_{INTRi} + 1 - \frac{\omega_{pi}^2}{\omega^2 + i\omega \left( \gamma_{mi} + \left( \frac{3v_{fi}}{4R_i} \right) \right)} \quad (5)$$

Where

$\gamma_{mi}$  is the macroscopic damping constant due to the dispersion of the electrons by the ions of the system of metallic inclusion,  $R_i$  is metallic inclusion radius,  $\omega_{pi}$  is the plasma angular frequency,  $v_{fi}$  is the fermi velocity of metallic inclusion.  $\epsilon_{INTRi}$  is the contribution from the intra-band transitions which can be calculated by the equation

$$\epsilon_{INTRi} = 1 - \frac{\omega_{pi}^2}{\omega^2 + i\omega(\gamma_{mi})} \quad (6)$$

The electron–hole pair generation rate in the nanocomposite absorber layer using individual metallic nanoparticles can be written as [2]

$$G_i(\lambda) = \frac{\alpha_{bi}(\lambda) e^{-\alpha_{wi}(d_w)} [1 - R(\lambda)] \lambda I_o(\lambda)}{hc} \quad (7)$$

Where,  $\lambda$  is the wave length,  $I_o(\lambda)$  is the intensity of the solar spectral,  $c$  is the speed of light,  $h$  is the Plank constant.  $\alpha_{bi}(\lambda)$  is the absorption coefficient of the absorber layer using individual nanoparticles  $\alpha_{wi}$  is the absorption coefficient of the window layer in nanocomposite thin film solar cells.

$\alpha_b(\lambda)$  and  $\alpha_w$  are the absorption coefficient of the absorber or window layer that can be calculated by the Beer-Lambert's law as following expression [21,22]

$$\alpha(\lambda) = \frac{2.303 \times A_t}{d_t} \quad (8)$$

$A_t$  is the absorbance of the absorber or window layer that calculated by the following expression [22]

$$A_t = 1 - T_{tef} - R_{tef} \quad (9)$$

Where

$d_t$  is the thickness of the layer,  $R_{tef}$  and  $T_{tef}$  are the reflectance and transmittance of layer that evaluated from the following equation [23]

$$R_{tef} = \frac{p^2 + Z^2 + 2pZ\cos\theta}{1 + 2p^2Z^2 + 2pZ\cos\theta} \quad (10)$$

The transmittance of the film has been derived as

$$T_{tef} = \frac{16n_o^2 n_t^2 n_s}{1 + 2p^2Z^2 + 2pZ\cos\theta} \quad (11)$$

Where

$$p = \frac{n_o - n_t}{n_o + n_t}, \quad Z = \frac{n_t - n_s}{n_t + n_s} \quad \theta = \frac{4\pi n_t d_t}{\lambda} \quad (12)$$

Where

$\lambda$  is wave length,  $n_0$  is refractive index of air,  $n_s$  is the refractive index of substrate film layer material

$n_t$  is the refractive index of thin film layer material. The reflectance of front layer in thin film solar cell  $R(\lambda)$  in equation (9) was evaluated using equation (12). The refractive index of front layer material (SnO<sub>2</sub> or ITO) calculated material calculated using sellmeier equations [24-26]. whatever, the refractive index of thin film window layer (CdS) as substrate film doping semiconductor for front layer or as thin film layer materials are calculated as follows [27]:

$$n = \sqrt{\frac{|\epsilon_b| + \epsilon_{reb}}{2}} \quad (13)$$

The refractive index of nanocomposite absorber material (CdTe, PbS) using individual nanoparticles calculated by the equation [27]

$$n_{fi} = \sqrt{\frac{|\epsilon_{efi}| + \epsilon_{refi}}{2}} \quad (14)$$

Where,  $\epsilon_{refi}$  is the real part of the effective dielectric constant of nanocomposite absorber layer material,  $|\epsilon_{efi}|$  is the absolute value of the effective dielectric constant of nanocomposite absorber layer material. The substrate layer material of absorber layer is metallic material (Cu, Al). The dielectric constant of the metallic material  $\epsilon_m$  can be described as [18].

$$\epsilon_m = \epsilon_{INTRA} + 1 - \frac{\omega_m^2}{\omega^2 + i\omega(\gamma_m)} \quad (15)$$

Where,  $\gamma_m$  is the macroscopic damping constant due to the dispersion of the electrons by the ions of the system of metallic inclusion.  $\omega_m$  is the plasma angular frequency,  $\epsilon_{INTRA}$  is the contribution from the intra-band transitions which can be calculated by Eq. 8 by using  $\gamma_m$ ,  $\omega_m$  for metallic substrate layer material. The refractive index of substrate film absorber layer materials is calculated by using Eq. 16 by using dielectric constant of metallic material  $\epsilon_m$ .

The photocurrent density for the carriers drifting towards the top contact using individual nanoparticles become [2].

$$J_{ni}(\lambda.V) = \frac{QG_iW_i}{\left(\frac{1}{\check{v}_i} - \frac{1}{\psi_i}\right)} \left[ \psi_i \left(1 - e^{\frac{-1}{\psi_i}}\right) - \check{v}_i \left(1 - e^{\frac{-1}{\psi_i} \frac{1}{\check{v}_i}}\right) \right] \quad (16)$$

The photocurrent density for the carriers drifting towards the bottom contact using individual nanoparticles become [2]

$$J_{li}(\lambda.V) = \frac{QG_iW_i}{\left(\frac{1}{\check{\epsilon}_i} - \frac{1}{\psi_i}\right)} \left[ \psi_i \left(1 - e^{\frac{-1}{\psi_i}}\right) - \check{\epsilon}_i \left(1 - e^{\frac{-1}{\check{\epsilon}_i}}\right) \right] \quad (17)$$

Where

$\psi_i$ ,  $\check{\epsilon}_i$ ,  $\check{v}_i$  are the normalized absorption depth, the normalized carrier lifetime (carrier lifetime per unit transit time) for the carriers drifting towards the bottom contact and the normalized carrier Lifetime (carrier Lifetime per unit transit time) for the carriers drifting towards the top contact that calculated by

$$\psi_i = \frac{1}{\alpha_{bi}W_i}, \quad \check{\epsilon}_i = \frac{\mu_{bt}F_i}{W_i}, \quad \check{v}_i = \frac{\mu_{tt}F_i}{W_i} \quad (18)$$

where t and b refer to the carrier type

The external voltage dependent electric field is given by [2,28],

$$F_i = \frac{V_{bi} - (V - J(V)R_{ser})}{W_i} \quad (19)$$

Whatever,  $J_{diode}(V)$  is the forward diode current for nanocomposite cells using individual nanoparticles as in ref. [2,28-31]:

$$J_{diode}(V) = J_{oi} \left[ \exp\left(\frac{Q(V + J(V)R_{ser})}{nKT}\right) - 1 \right] \quad (20)$$

$$J_{oi} = \frac{W_i Q \sqrt{N_{con} N_{val}} \exp\left(-\frac{E_{gbi}}{KT}\right)}{\sqrt{\tau_e \tau_h}} \quad (21)$$

$$W_i = \sqrt{\frac{2\epsilon_0 \epsilon_{efi} (V_{bi} - V)}{Q(N_a - N_d)}} \quad (22)$$

Where,  $V_{bi}$  is the built-in potential.  $N_a$  is the acceptor carrier concentration by using individual nanoparticles.  $V$  is the applied voltage.  $J_{oi}$  is reverse saturation current density in nanocomposite cells.  $N_{con}$ ,  $N_{val}$  is the effective state densities in the conduction and valence bands.  $R_{ser}$  is the series resistance.  $n$  is diode ideality factor.  $T$  is absolute temperature.  $K$  is boltzman constant.  $\tau_e$  is the electron lifetime.  $\tau_h$  is the hole lifetime.

Note that,  $N_{con}$  depend on the effective mass of electron [4,32].

$E_{gbi}$  is the energy band gap of nanocomposites absorber layer material that has been affected by the metallic nanoparticles. The energy band gap of a semiconductor increases with decreasing dielectric constant according with respect to various empirical rules and expressions of refractive index and energy band gap [15,32-34].

Many attempts have been made to correlate the energy band gap to the optical refractive index of semiconductors. Moss was the first to find a relation between the refractive index  $n$  and the energy band gap  $E_g$ . Ravindra and Srivastava suggested another relation. Reddy and Anjaneyulu proposed alogarithmical form of  $n$  as afunction of  $E_g$ . Herve'and Vandamme proposed an overall relation based on theclassical oscillator theory. Based on Reddy and Anjaneyulu formula, the energy band gap of nanocomposites absorber layer material  $E_{gbi}$  has been calculated by the following expression [35-37]:

$$E_{gbi} = \frac{36.3}{e^{n_{fi}}} \quad (23)$$

The resultant photocurrent density  $J_{Ti}(\lambda.V)$  calculated by the expression [2]

$$J_{Ti}(\lambda.V) = J_{li}(\lambda.V) + J_{ni}(\lambda.V) \quad (24)$$

$J_{phi}(V)$  is total photo generated current density using individual nanoparticles which obtained by integrating over all incident photon wavelengths of the solar spectrum [2]

$$J_{phi}(V) = \int_0^{\infty} J_{Ti}(\lambda.V) d\lambda \quad (25)$$

The net external current density from a solar cell using individual nanoparticles is [2,31]

$$J_{ind}(V) = J_{phi}(V) - J_{diode}(V) - \left( \frac{V + J_{ind}(V)R_{ser}}{R_{sh}} \right) \quad (26)$$

Where,  $R_{sh}$  is the shunt resistance

The open circuit voltage equation is expressed as [30].

$$V_{oci} = \left( \frac{KT}{Q} \right) \ln \left[ \frac{J_{phi}}{J_0} + 1 \right] \quad (27)$$

The output power density from solar cell using individual nanoparticles calculated by the following equation [4]

$$p_{ind} = J_{ind} \times V \quad (28)$$

The calculation of fill factor to an excellent accuracy [4],

$$Fill\ Factor = \frac{P_{max}}{V_{oci} \times J_{phi}} \quad (29)$$

$P_{max}$  is the maximum point of output power density which calculate from p-v curve.

The final equation for the efficiency of the solar cell is [16]

$$n_i = \frac{J_{phi} V_{oci} Fill\ Factor}{P_{in}} \times 100 \quad (30)$$

The external quantum efficiency  $EQE_i(\lambda)$  is defined as the ratio of electrical charges extracted from a solar cell to the number of incident photons. It has been calculated by the following equation [38-40]

$$EQE_i(\lambda) = \frac{J_{phi}(\lambda)}{Q\phi(\lambda)} \quad (31)$$

Where,  $P_{in}$  is the intensity of the incident radiation,  $\phi(\lambda)$  is the spectral photon density

### III. SPECIFICATIONS OF METALLIC MATERIALS AND NANOCOMPOSITES MODELS

Knowledge of specifications of magnetic materials is the first step for designing new nanocomposites thin film solar cell with high J-V and P-V characteristics. The proposal models used the parameters which achieve the efficiency and J-V characteristics of previous practical (ITO/CdS/PbS/Al, SnO<sub>2</sub>/CdS/CdTe/Cu). models, also; The proposal models used the thicknesses of the selected previous practical models [3,4]. Tables depict the main parameters of usage materials and parameters of nanocomposites thin film models;

TABLE I  
CHARACTERISTICS PARAMETERS OF USAGE MATERIALS IN NANOCOMPOSITES THIN FILM SOLAR CELLS MODELS [16,17, 41,42]

Parameters	CdTe	PbS	CdS
Band gap (eV) at zero Kelvin	1.6077	0.543	2.58
Band gap parameter $\alpha$ (eV.K <sup>-1</sup> ) × 10 <sup>-4</sup>	3.1	5	4.202
Band gap parameter $\beta$ (K)	108	0.40	147
Electron mobility (cm <sup>2</sup> /Vs)	320	1000	350
Hole mobility (cm <sup>2</sup> /Vs)	40	80	50
Effective mass of electron	0.11	0.1	0.2
Effective mass of holes	0.35	0.1	0.7

TABLE II  
PARAMETERS OF USAGE THIN FILM SOLAR CELLS MODELS [3,4]

Parameters	SnO <sub>2</sub> /CdS/CdTe/Cu	ITO/CdS/PbS/Al
Absorber layer thickness (nm)	500	500
Window layer thickness (nm)	100	100
Front layer thickness (nm)	100	100
Electron lifetime (s)	1 × 10 <sup>-8</sup>	10 <sup>-9</sup>
Hole lifetime (s)	5 × 10 <sup>-8</sup>	10 <sup>-9</sup>
$N_a - N_d$ the concentration of uncompensated acceptors (cm <sup>-3</sup> )	2.44 × 10 <sup>12</sup>	0.19 × 10 <sup>10</sup>
Diode quality factor	1.6	1.4
Series resistance ( $\Omega$ . Cm <sup>2</sup> )	1.08	2.1
Shunt resistance ( $\Omega$ . Cm <sup>2</sup> )	103	204

The aim of our work to improve the efficiency and performance of practical models of previous work to achieve high efficiency with less absorber layer thickness to save the materials which decrease the cost; the results have been obtained using nanometallic fillers radii 1nm and under illumination condition of AM1.5 solar irradiation.

TABLE III  
CHARACTERISTICS OF USAGE MATERIALS AS SUBSTRATE LAYER OR FILLERS IN ABSORBER LAYER FOR NANOCOMPOSITES THIN FILM MODELS [43-46]

Material	Plasma angular frequency ( $\omega_p$ , 10 <sup>16</sup> rad/s)	Damping constant ( $\gamma_m$ , 10 <sup>13</sup> s <sup>-1</sup> )	Fermi velocity ( $v_f$ , 10 <sup>6</sup> m/s)
CdTe	0.052	8.88	-
PbS	0.014	1.76	-
Cesium (Cs)	0.54	0.756	0.75
Lithium (Li)	1.225	1.85	1.29
Copper (Cu)	1.03	5.26	1.57
Silver (Ag)	1.40	2.80	1.39
Aluminum (Al)	1.09	12.4	2.03
Molybdenum (Mo)	0.19	1.13	-

IV. RESULTS AND DISCUSSION

Figure 1 depicts the refractive index and dielectric constant of CdTe nanocomposites with various volume fractions. The refractive index and dielectric constant of CdTe nanocomposites decreased by increasing the concentration of Silver, Copper, Lithium, Aluminum or Cesium metallic nanofillers in the CdTe base matrix. Fig 2 depicts the energy band gap of CdTe nanocomposites with various volume fractions. The energy band gap of CdTe enhanced by increasing the volume fraction. Cesium has been the best inclusion used for increasing the energy band gap of CdTe.

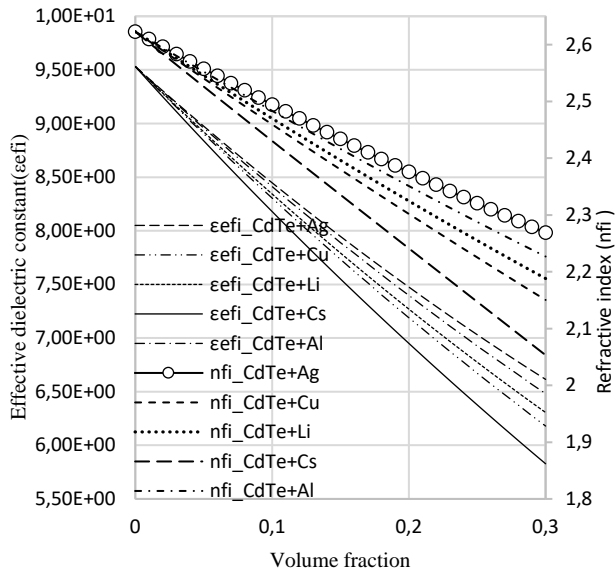


Fig. 1: Dielectric constant and refractive index of CdTe nanocomposites with various volume fractions

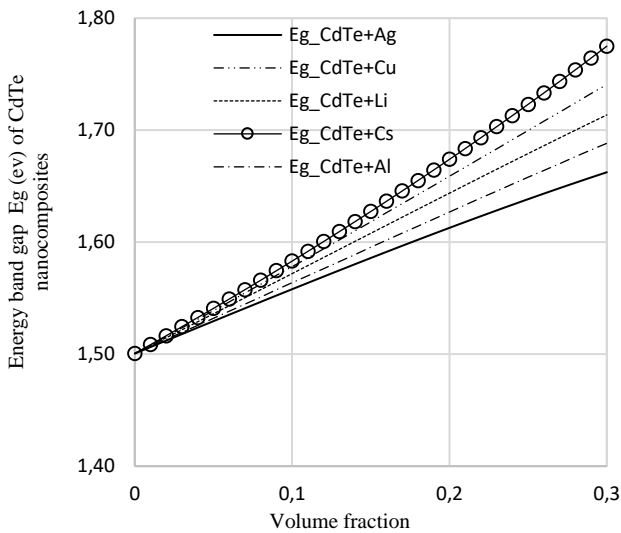


Fig. 2: Effect of metallic nanoparticles on the energy band gap of CdTe

Figure 3 illustrates the inclusions radii effect on absorption coefficient of CdTe nanocomposites layer. The absorption coefficient of CdTe nanocomposites increased with increasing radii of selected metallic nanoparticles.

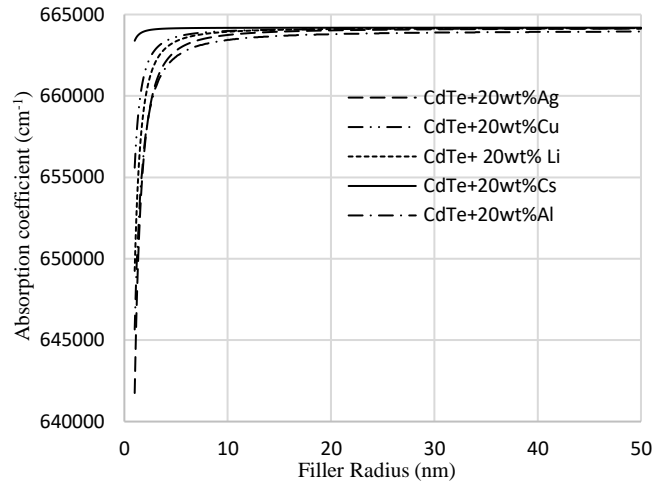


Fig. 3: Metallic nanoparticles radii effect on absorption coefficient of CdTe nanocomposites layer

Figures 4,5 shows J-V and P-V characteristics of SnO<sub>2</sub>/CdS/CdTe/Cu nanocomposites thin film solar cells using individual nanoparticles. Using 20wt.% of Silver, Copper, Lithium, Aluminum or Cesium individual nanoparticles in CdTe absorber layer enhanced the short circuit current density, open circuit voltage and output power density of CdS/CdTe nanocomposites thin film solar cell. Using 20wt.%Cesium nanoparticles in absorber layer has been the best inclusion for improving the J-V and P-V characteristics of SnO<sub>2</sub>/CdS/CdTe/Cu nanocomposites thin film solar cell at room temperature.

Figure 6 describes the external quantum efficiency of SnO<sub>2</sub>/CdS/CdTe/Cu nanocomposites thin film solar cells using individual nanoparticles. Using 20wt.% of metallic nanoparticles (Copper, Lithium, Cesium, Aluminum and Silver) enhanced the external quantum efficiency of CdS/CdTe nanocomposites thin film solar cells with increasing the wave length. Figure 7 shows the metallic nanoparticles concentration effect on depletion width of SnO<sub>2</sub>/CdS/CdTe/Cu nanocomposites thin film solar cell. The increase in the

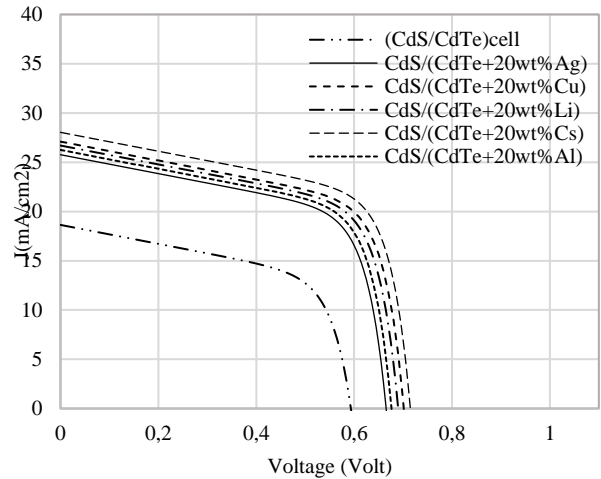


Fig. 4: J-V characteristics of SnO<sub>2</sub>/CdS/CdTe/Cu nanocomposites thin film solar cells using individual nanoparticles

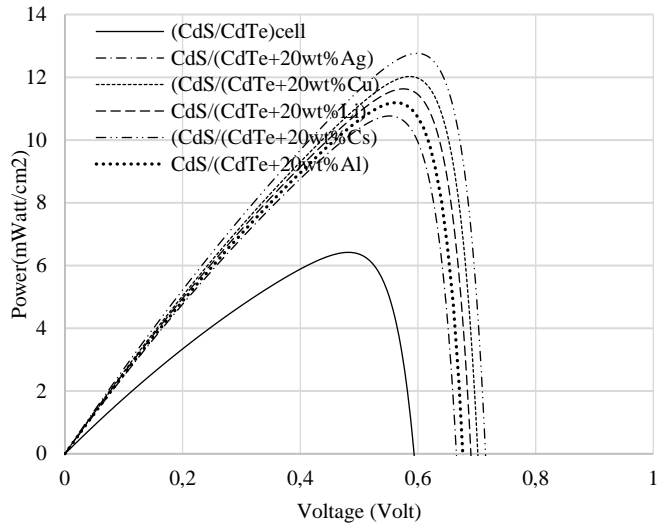


Fig. 5: P-V characteristics of SnO<sub>2</sub>/CdS/CdTe/Cu nanocomposites thin film solar cells using individual nanoparticles

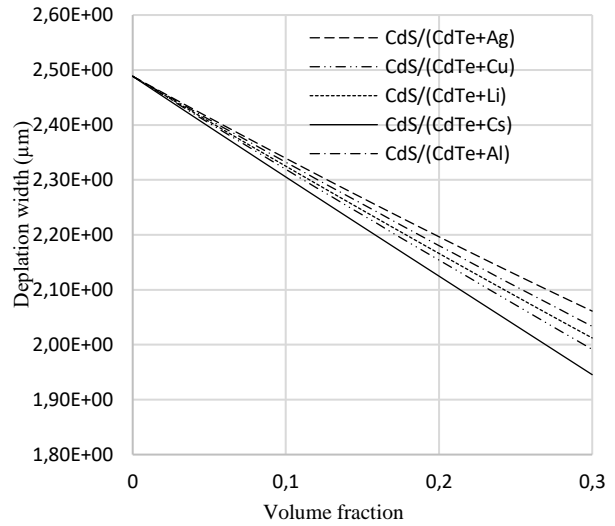


Fig. 7: Metallic nanoparticles concentration effect on depletion width of SnO<sub>2</sub>/CdS/CdTe/Cu nanocomposites thin film solar cell

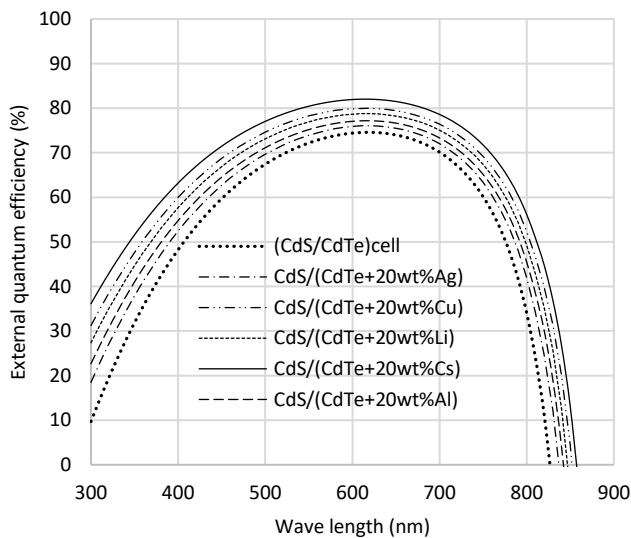


Fig. 6: External quantum efficiency of SnO<sub>2</sub>/CdS/CdTe/Cu nanocomposites thin film solar cells using individual nanoparticles

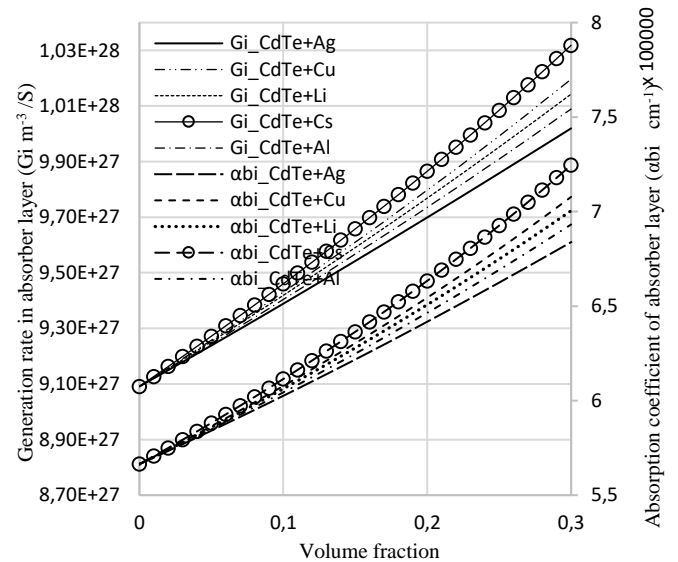


Fig. 8: Metallic nanoparticles concentration effect on the generation rate and absorption coefficient in absorber layer of SnO<sub>2</sub>/CdS/CdTe/Cu nanocomposites thin film solar cell

concentration of metallic nanoparticles in the absorber layer CdS/CdTe thin film solar cell decreased the depletion width of CdS/CdTe nanocomposites thin film solar cell. Cesium has been the best inclusion used for decreasing the depletion width of CdS/CdTe nanocomposites thin film solar cell. Copper has been the second order for decreasing the depletion width of cell. However, Silver has been the least one for decreasing the space charge region.

Figure 8 shows the metallic nanoparticles concentration effect on the generation rate and absorption coefficient in absorber layer of CdS/CdTe nanocomposites thin film solar cell. The generation rate has been enhanced by increasing the concentration of Silver, Copper, Lithium, Cesium, aluminum metallic nanoparticles in CdTe absorber layer of CdS/CdTe thin film solar cell. On the other side, The absorption coefficient of CdTe nanocomposites layer increased by increasing the concentration of Silver, Copper, Lithium, Aluminum or Cesium metallic nanofillers in the CdTe base matrix layer.

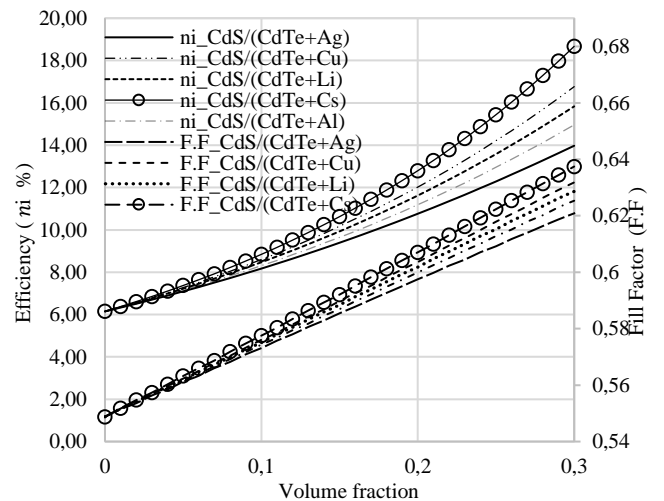


Fig. 9: Metallic nanoparticles concentration effect on the fill factor and efficiency of SnO<sub>2</sub>/CdS/CdTe/Cu nanocomposites thin film solar cell

Figure 9 shows the metallic nanoparticles concentration effect on the energy conversion efficiency and fill factor of CdS/CdTe nanocomposites thin film solar cells. The figure shows that the increase in the concentration of metallic nanoparticles in the absorber layer of CdS/CdTe nanocomposites thin film solar cells increased the efficiency and fill factor of CdS/CdTe nanocomposites thin film solar cell. Cesium has been the best filler for increasing the efficiency of CdS/CdTe nanocomposites thin film solar cell, however; Silver has been the least one for enhancing the energy conversion efficiency and fill factor of the cells.

Figure 10 show the dielectric constant and refractive index of PbS nanocomposites with various volume fractions. The increase in the concentration of Silver, Copper, Lithium, Cesium or Aluminum nanometallic particles in PbS base matrix decreased the dielectric constant and refractive index of PbS with increasing the volume fraction. Cesium has been the best inclusion for decreasing the refractive index and dielectric constant of PbS. On the other side, fig 11 describes the effect of metallic nanoparticles on the energy band gap of PbS. Adding metallic nanoparticles of Aluminum, Lithium, Cesium, Copper or silver in PbS base matrix enhanced the energy band gap of PbS with increasing the volume fraction.

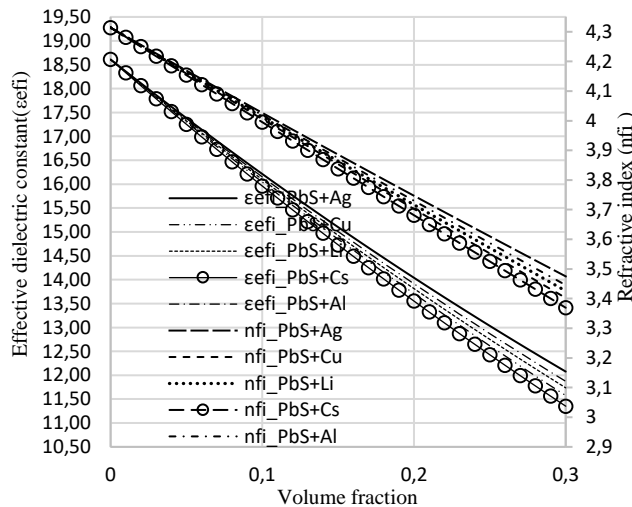


Fig. 10: Dielectric constant and Refractive index of PbS nanocomposites with various volume fractions

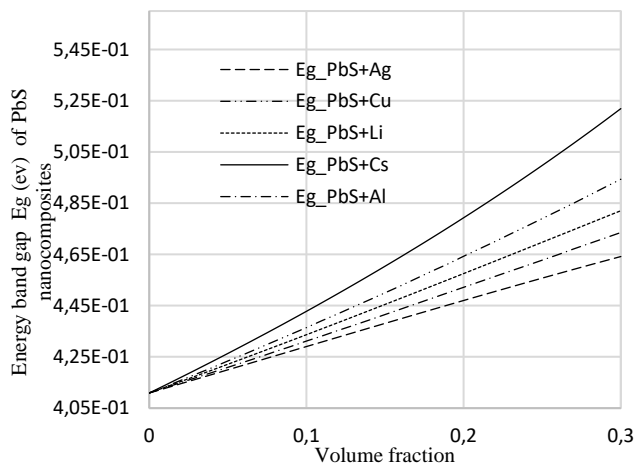


Fig. 11: Effect of metallic nanoparticles on the energy band gap of PbS

Figure 12 illustrates the inclusions radii effect on absorption coefficient of nanocomposites layer. The absorption coefficient of PbS nanocomposites increased with increasing radii of selected metallic nanoparticles.

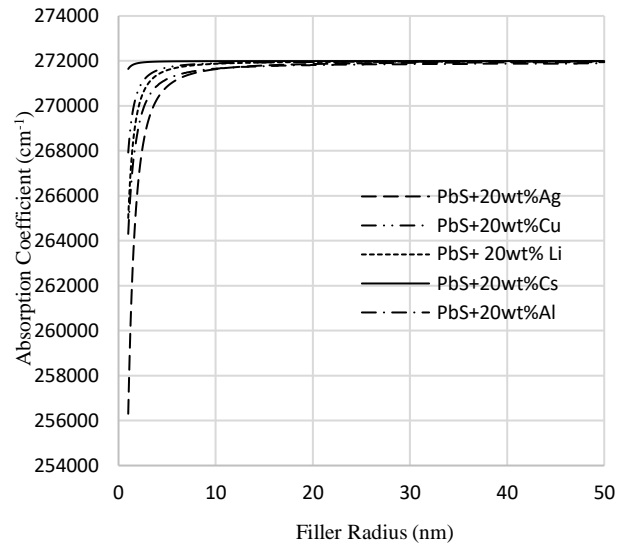


Fig. 12: Metallic nanoparticles radii effect on absorption coefficient of PbS nanocomposites layer

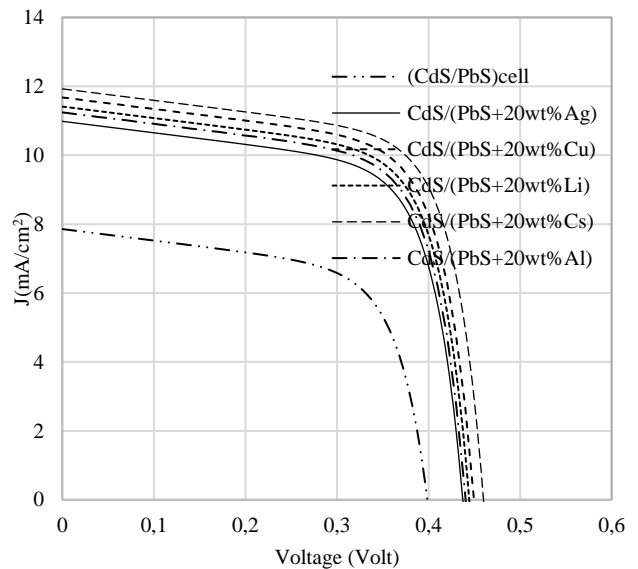


Fig. 13: J-V characteristics of ITO/CdS/PbS/Al nanocomposites thin film solar cells using individual nanoparticles

Figures 13,14 obvious the J-V and P-V characteristics of ITO/CdS/PbS/Al nanocomposites thin film solar cells using individual nanoparticles. Adding 20wt.% of Silver, Copper, Lithium, Cesium or Aluminum metallic nanoparticles in PbS absorber layer enhanced the performance of the cell by increasing the short circuit current, open circuit voltage and output power density of ITO/CdS/PbS/Cu nanocomposites thin film solar cell. Cesium has been the first order for enhancing the J-V and P-V characteristics of CdS/PbS nanocomposites thin film solar cell. Copper has been the second order for enhancing the J-V and P-V characteristics of ITO/CdS/PbS/Al

nanocomposites thin film solar cell. Silver has been the least one for enhancing the J-V and P-V characteristics of CdS/PbS nanocomposites thin film solar cell.

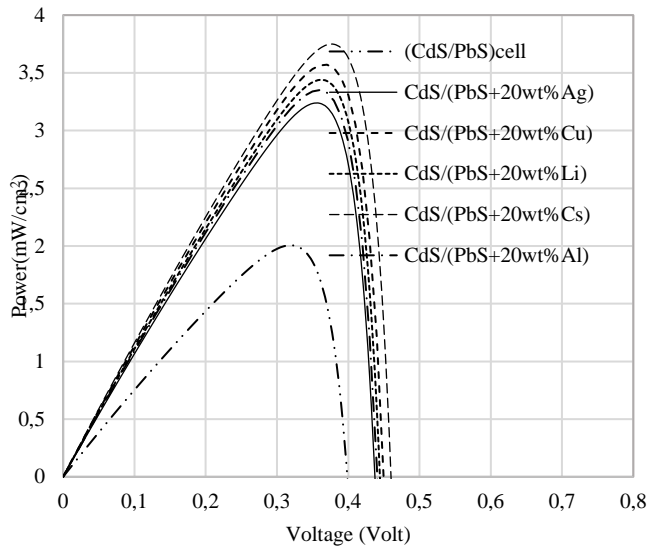


Fig. 14: P-V characteristics of ITO/CdS/PbS/Al nanocomposites thin film solar cells using individual nanoparticles

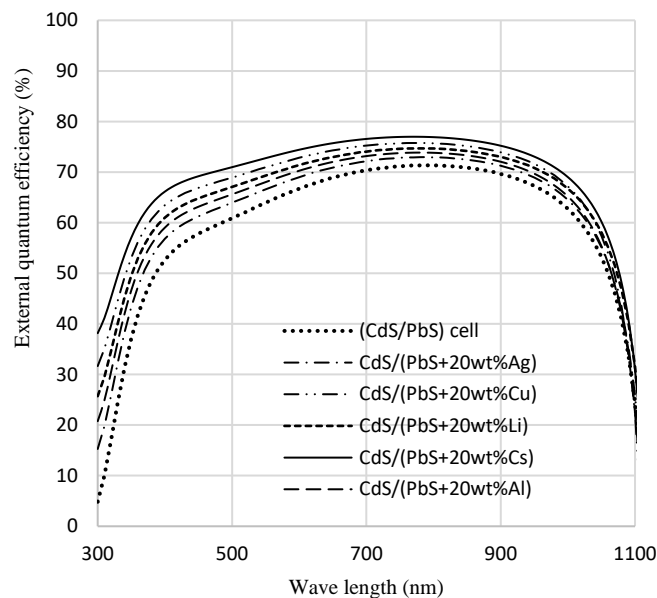


Fig. 15: External quantum efficiency of ITO/CdS/PbS/Al nanocomposites thin film solar cells using individual nanoparticles

On the Other hand, Fig. 15 describes the external quantum efficiency of ITO/CdS/PbS/Al nanocomposites thin film solar cells using individual nanoparticles. The external quantum efficiency of CdS/PbS nanocomposites thin film solar cells has been increased by using 20wt.% of Silver, Aluminum, Lithium, Copper or Cesium nanoparticles in the PbS absorber layer due to increasing the optical properties of PbS layer and decreasing the recombination of the cell. The most enhancements have

been occurred by using Cesium nanoparticles in the PbS absorber layer with increasing the wave length. Copper has been the second order for enhancing the external quantum efficiency of ITO/CdS/PbS/Al nanocomposites thin film solar cell. Whatever, Fig. 16 illustrates the metallic nanoparticles concentration effect on the electron-hole generation rate and absorption coefficient for absorber layer in ITO/CdS/PbS/Al nanocomposites thin film solar cell. Adding Silver, Copper, Aluminum, Cesium or Lithium individual metallic nanoparticles in PbS absorber layer increased the electron-hole pair generation rate in the absorber layer. The absorption coefficient of PbS nanocomposites layer increased by increasing the volume fraction. Using individual nanoparticles of Cesium, Aluminum, Copper, Lithium or Aluminum in PbS base matrix layer improving the absorption coefficient of layer with increasing the volume fraction. Cesium has been the best nanometallic for increasing the absorption coefficient, then; Copper has been the second order for improving the absorption coefficient. Silver has been the least one for improving the absorption coefficient of PbS layer.

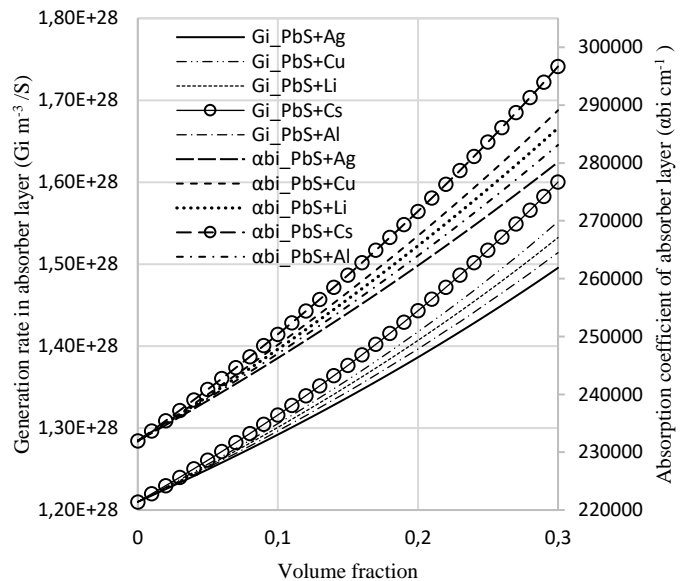


Fig. 16: Metallic nanoparticles concentration effect on the generation rate of ITO/CdS/PbS/Al nanocomposites thin film solar cell

Figure 17 shows the metallic nanoparticles concentration effect on depletion width of ITO/CdS/PbS/Al nanocomposites thin film solar cell. the figure show that the depletion region decreased by increasing the volume fraction of Lithium, Copper, Aluminum, silver or Cesium individual nanoparticles. In case of Fig. 18 that shows the metallic nanoparticles concentration effect on the efficiency and fill factor of CdS/PbS nanocomposites thin film solar cell. Anew solar cell design that using individual nanoparticles of Silver, Copper, Lithium, Aluminum or Cesium in PbS absorber layer could raise the energy conversion efficiency and fill factor of CdS/PbS nanocomposites thin film solar cell with increasing the volume fraction.



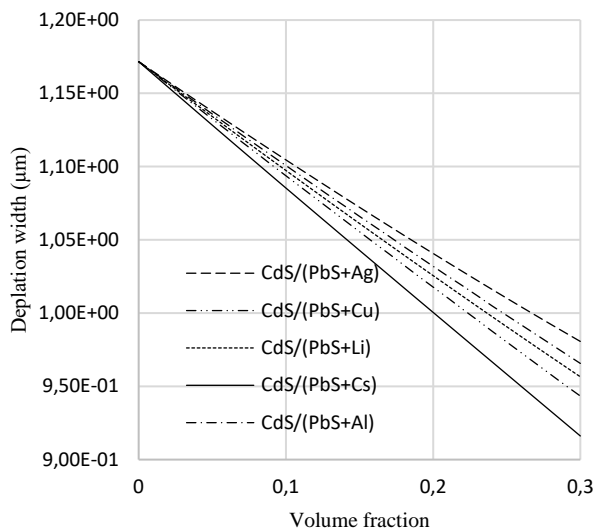


Fig. 17: Metallic nanoparticles concentration effect on depletion width of ITO/CdS/PbS/Al nanocomposites thin film solar cell

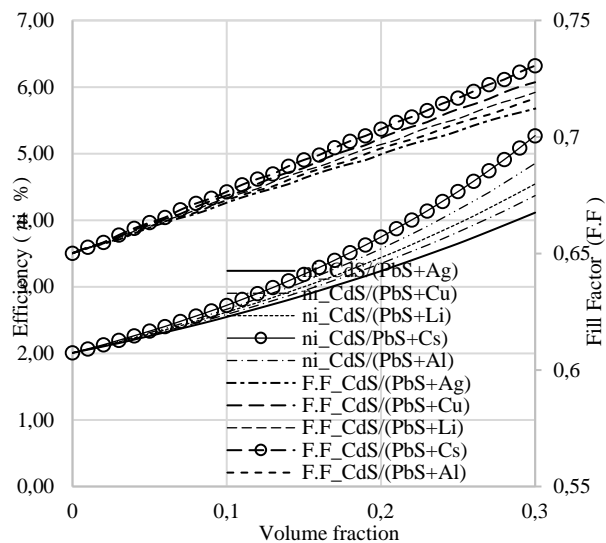


Fig. 18: Metallic nanoparticles concentration effect on the efficiency and fill factor of ITO/CdS/PbS/Al nanocomposites thin film solar cell

### CONCLUSION

- The dielectric constant and refractive index of CdTe or PbS nanocomposites decreased by increasing the concentration of Silver, Copper, Lithium, Aluminum or Cesium metallic nanofillers in the CdTe or PbS base matrix. On the other side, the energy band gap of CdTe or PbS has been enhanced by increasing the volume fraction of selected metallic nanoparticles.
- Using individual nanoparticles of Silver, Copper, Lithium, Aluminum or Cesium enhanced the absorption coefficient of CdTe or PbS layers with increasing the volume fraction.
- The absorption coefficient of CdTe or PbS nanocomposites layers increased with increasing radii of Silver, Copper, Lithium, Aluminum or Cesium metallic nanoparticles below

radii 10nm. After radii 10nm the enhancement in the absorption coefficient of CdTe or PbS nanocomposites layers decreased, then the absorption coefficient of selected semiconductor layers has been constant with increasing radii of metallic fillers.

- Using 20wt.% of Silver, copper, Lithium, Aluminum or Cesium individual nanoparticles in CdTe or PbS absorber layers enhanced the short circuit current density, open circuit voltage, output power density and external quantum efficiency of CdS/CdTe or CdS/PbS nanocomposites thin film models based on sub micro absorber layer thickness. The increase in the concentration of Cesium, Silver, Lithium, Aluminum or Copper individual metallic nanoparticles in the absorber layer of CdS/CdTe or CdS/PbS nanocomposites thin film models improved the performance of models by decreasing the space charge region and increasing the electron-hole pair generation rate in the absorber layer and the efficiency and fill factor of models.
- Using Cesium as individual nanoparticles has been the best for improving the performance of ITO/CdS/PbS/Al and  $\text{SnO}_2/\text{CdS}/\text{CdTe}/\text{Cu}$  nanocomposites thin film solar cells.

### REFERENCES

- [1] LEE T., A. EBONG. A review of thin film solar cell technologies and challenges. *Renewable and Sustainable Energy Reviews*. Elsevier. 2016, Vol. 12. DOI: 10.1016/j.rser.2016.12.028.
- [2] MANNAN M., M.S. ANJAN, M.Z. KABIR, Modeling of current-voltage characteristics of thin film solar cells. Elsevier. 2011, Vol. 6. DOI: org/10.1016/j.sse.2011.05.010
- [3] BAI Z., J. YANG, S. DEPBA, D. WANG, Thin film CdTe solar cells with an absorber layer thickness in micro- and sub-micrometer scale. *Applied Physics Letters*. 2011, Vol. 4. DOI: org/10.1063/1.3644160
- [4] MOHAMED H. Theoretical study of the efficiency of CdS/PbS thin film solar cells. Elsevier. 2014, Vol. 10. DOI: org/10.1016/j.solener.2014.07.017
- [5] HUI P., R. ELISABETH, M. VEHSE. Cost-effective nanostructured thin-film solar cell with enhanced absorption. *Applied Physics Letters*. 2014, Vol. 7. DOI: org/10.1063/1.4901167
- [6] KRISHNAKUMAR V, A. BARATI, H. J. SCHIMPER, A. KLEIN, AND W. JAEGERMANN. A possible way to reduce absorber layer thickness in thin film CdTe solar cells. *Thin Solid Films*. 2013, pp.535, 233. DOI: 10.1016/j.tsf.2012.11.085.
- [7] PIRALAE M, A. ASGARI, Modeling of optimum light absorption in random plasmonic solar cell using effective medium theory. Elsevier. 2016, Vol. 4. DOI: org/10.1016/j.optmat.2016.10.021.
- [8] NOTTLE D. Optical scattering and absorption by metal nanoclusters in GaAs. 1994, Vol. 6. DOI: org/10.1063/1.357445.
- [9] VLADIMIR M. Optical Properties of Nanostructured Random Media. Springer, 2002. DOI: 10.1007/3-540-44948-5
- [10] HAMAGUCHI C. Basic semiconductor physics. 2<sup>nd</sup> edition. Springer. 2010, pp. 201. DOI: 10.1007/978-3-642-03303-2
- [11] JIMENEZ J., W. Tomm. Spectroscopic Analysis of optoelectronic semiconductors. Springer series in optical science. 2016, Pp. 27. DOI: 10.1007/978-3-319-42349-4
- [12] HARRISON P., Quantum wells, wires and dots: Theoretical and computational physics of semiconductor nanostructures. 3<sup>rd</sup> edition. Wiley Interscience. 2011, ch.13. ISBN: 978-1-119-96475-9
- [13] FOX M., Optical properties of solids. 2<sup>nd</sup> edition. 2010, Pp.187. ISBN: 9780199573370.
- [14] KON H, B. RIEGER. IAENG transactions on engineering technologies. 2013, Pp. 45. DOI: 10.1007/978-94-007-4786-9

- [15] RIDLEY B. Quantum processes in semiconductors. 2013, Ch.16, Pp. 418. ISBN: 0191664898.
- [16] SINGH P., N. RAVINDRA. Temperature dependence of solar cell performance -an analysis. Elsevier. 2012. Vol. 10. DOI: 10.1016/j.solmat.2012.02.019.
- [17] RAVINDRA N., S. AULUCK, V. SRIVASTAVA. Temperature dependence of the energy gap in PbS, PbSe, and PbTe. *physica status solidi*. 1979, Vol. 5. DOI: org/10.1002 /pssa. 2210 520255.
- [18] NOGUEZ C. Optical properties of isolated and supported metal nanoparticles. Elsevier. 2005, Vol. 8. DOI: org/10.1016/j.optmat.2004.11.012
- [19] C. NOGUEZ. Surface plasmons on metal nanoparticles: the influence of shape and physical environment. *J. Phys. Chem. C*, 2007, Vol.14. DOI: 10.1021/jp066539m.
- [20] SAU T., A. ROGACH. Complex shaped metal nanoparticles. 2012, Pp. 369. DOI: 10.1002/978 3527652570
- [21] GHOBADI N. Band gap determination using absorption spectrum fitting procedure. Springer. 2013, Vol. 4. DOI: 10.1186/2228-5326-3-2
- [22] DAS R., S. PANDEY, Comparison of optical properties of bulk and nanocrystalline thin films of CdS using different precursors. *International Journal of Material Science*. 2011, Vol. 6. Iss.1. PP.35-40.
- [23] SULTAN M., N. SULTANA. Analysis of reflectance and transmittance characteristics of optical thin film for various film materials, thicknesses and substrates. *J Electr Electron Sys*. 2015, Vol. 4. DOI:10.4172/2332-0796.1000160
- [24] PALIK E., Handbook of optical constants of solids: handbook of thermo-optic coefficient of optical materials with applications. Elsevier. 1997, Pp.11. ISBN: 978-0-12-544415-6
- [25] YANG Y., X. SUN, B.J. CHEN, T. CHEN, C. SUN, B. TAY, Z. SUN. Refractive indices of textured indium tin oxide and zinc oxide thin films. Elsevier. 2006. DOI: 10.1016 /j.tsf.2005. 12.265.
- [26] SHANNONA R., O. MEDENBACHB, R. FISCHERC. Refractive Index and Dispersion of Fluorides and Oxides. *J. Phys. Chem. Ref. Data*. 2002, Vol. 31, No. 4. DOI: org/10.1063 /1.149 7384
- [27] FREDERICK W. Optical properties of solids. 1972, Pp. 49. ISBN: 1483207331
- [28] E. TAWSIF A., ANJUM, M. TANZIDUL. Parametric analysis of CdTe/CdS thin film solar cell. *International Journal of Advanced Research in Computer and Communication Engineering*. 2016, Vol. 5. DOI: 10.17148/IJARCC.2016. 5684.
- [29] MISHRA U., J. SINGH. Semiconductor device physics and design. Netherlands: Springer, 2008. [chapter 4]. ISBN 978-1-4020-6481-4
- [30] S. PUSPITA., S. HOQUE, M. SHAMIM. Theoretical efficiency and cell parameters of AlAs/GaAs/Ge based new multijunction solar cell. *IEEE*. 2016, Vol. 6. DOI: org/10.1109/CEEICT .2016.7873128
- [31] PRAKASH R., S. SINGH. Designing and modelling of solar photovoltaic cell and array. *IOSR Journal of Electrical and Electronics Engineering (IOSR-JEEE)*. 2016, pp 35-40Vol. 6. e-ISSN: 2278-1676,p-ISSN: 2320-3331.
- [32] VAN B., Principles of semiconductor devices. 2011. [bart@colorado.edu](mailto:bart@colorado.edu)
- [33] EL-NAHASS M., G. M. YOUSSEF and Z. SOHAIL. Structural and optical characterization of CdTe quantum dots thin films. Elsevier. 2014, Vol. 7. DOI: org/10.1016/j.jallcom.2014.03.104.
- [34] SINGH J., Optical properties of condensed matter and applications. John Wiley & Sons, Ltd, 2006. DOI:10.1002/0470021942
- [35] ATTIA A., M.M. EL-NAHASS. M.Y. EL-BAKRY AND D.M. HABASHY. Neural networks modeling for refractive indices of semiconductors. *Optics Communications*. 2013, DOI: 10.1016/j.optcom.2012.09.016.
- [36] TRIPATHY S., "Refractive indices of semiconductors from energy gaps", *Optical Materials*. Elsevier, Vol. 7, 2015. <http://dx.doi.org/10.1016/j.optmat.2015.04.026>
- [37] REDDY R., ANJANEYULU S., " Analysis of the Moss and Ravindra relations, *Physica Status Solidi, Basic solid state physics*. P.P 17. 1992. DOI: org/ 10.1002/pssb. 2221740238
- [38] MOHAMED H., Enhancing the performance of thin film CdS/PbS photovoltaic solar cells. *Philosophical Magazine*. 2014. Vol. 22. DOI: org/10.1080/14786435.2014.961586
- [39] GHOSH H, S. MITRA, S. DHAR AND A. NANDI. Light-harvesting properties of embedded tin oxide nanoparticles for partial rear contact Silicon solar cell. Springer Science. 2016, Vol. 12. DOI: org/10.1007/s11468-016-0443-7
- [40] Blazev A., Photovoltaics for commercial and utilities power generation. 2013, ch.1. ISBN. 9781304233240
- [41] SAFA R., A. NEWAZ, M. ASADUZZAMAN, M. MAKSUDUR and K. AHMED. Numerical dataset for analyzing the performance of a highly efficient ultrathin film CdTe solar cell. Elsevier. 2017. Vol.5. DOI: org/10.1016/j.dib.2017.04.015
- [42] WHITAKER J., The electronics handbook. 1996, Ch. 9. Pp.124. ISBN. 0849383455.
- [43] HANDBUSH G., Mo Molybdenum: Physical Properties, Part 2. *Electrochemistry* 8th edition. 2013, Pp. 62. DOI: 10.1007/978-3-662-09293-4
- [44] DULEY W., UV Lasers: Effects and Applications in Materials Science. 2005, Ch. 2. pp. 40. ISBN: 978-0521464987
- [45] MICHEAL F., Radiative heat transfer 3rd edition. 2013, Pp. 77. ISBN: 9780123869449
- [46] YANCHUK B., Laser Cleaning: Optical Physics. *Applied Physics and Materials Science*. 2002, Pp. 136. DOI: org/10.1142/495